

## Supporting Information

### **Mechanistic studies on the reaction between aquacobalamin and the HNO donor Piloty's acid over a wide pH range in aqueous solution**

Justyna Polaczek,<sup>a</sup> Harishchandra Subedi,<sup>b</sup> Łukasz Orzeł,<sup>a</sup> Lynn Lisboa,<sup>c</sup> Ruth B. Cink,<sup>c,d</sup>  
Grażyna Stochel,<sup>a</sup> Nicola E. Brasch<sup>c-e,\*</sup> and Rudi van Eldik<sup>a,f,g,\*</sup>

<sup>a</sup> Faculty of Chemistry, Jagiellonian University, Gronostajowa 2, 30-387 Krakow, Poland.

<sup>b</sup> Division of Health and Life Sciences, Piedmont Virginia Community College, 501  
College Drive, Charlottesville, VA 22902-7589, USA.

<sup>c</sup> School of Science, Auckland University of Technology, Auckland 1142, New Zealand. E-  
mail: [nbrasch@aut.ac.nz](mailto:nbrasch@aut.ac.nz)

<sup>d</sup> The Dodd Walls Centre for Quantum and Photonic Technologies, New Zealand.

<sup>e</sup> The Maurice Wilkins Centre for Molecular Biodiscovery, New Zealand.

<sup>f</sup> Nicolaus Copernicus University in Torun, 87-100 Torun, Poland.

<sup>g</sup> Department of Chemistry and Pharmacy, University of Erlangen-Nuremberg,  
Egerlandstrasse 1, 91058 Erlangen, Germany. E-mail: [rudi.vaneldik@fau.de](mailto:rudi.vaneldik@fau.de)

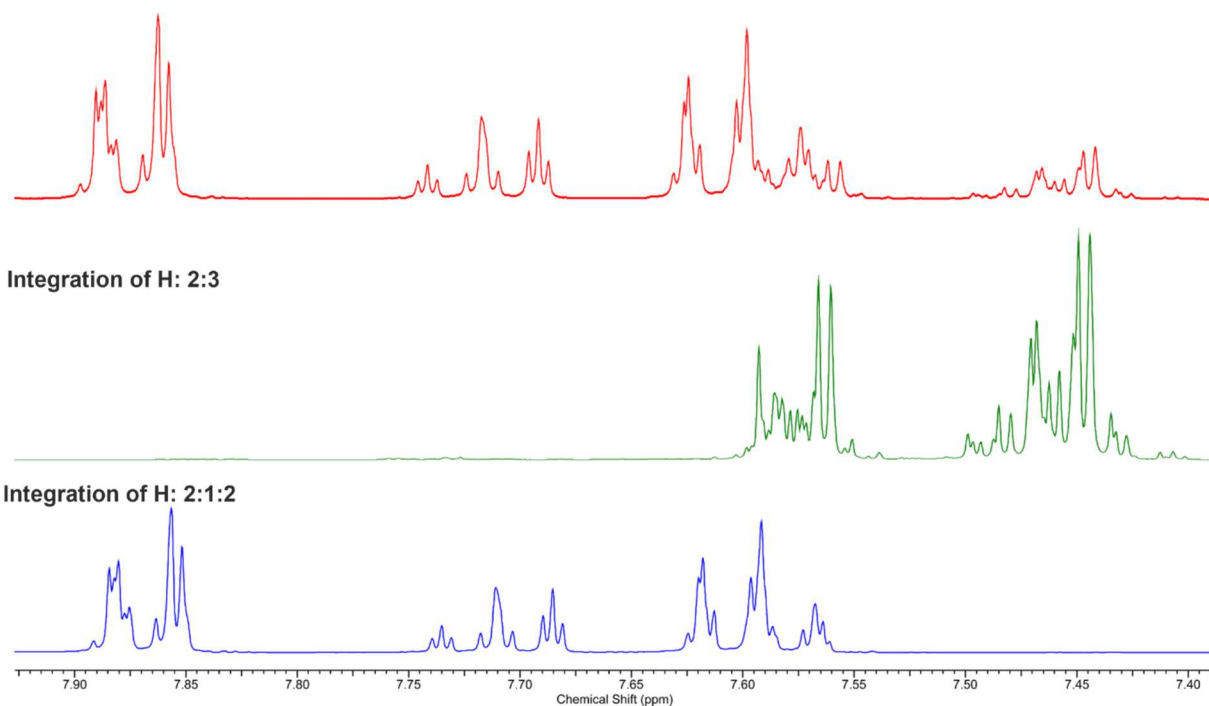


**Figure S1.** <sup>1</sup>H-NMR spectra recorded for Piloty's acid (blue spectrum) and benzenesulfinate (green spectrum), and a mixture of Piloty's acid and benzenesulfinate (10:1) (red spectrum) in D<sub>2</sub>O. The spectra clearly show that Piloty's acid does not contain any benzenesulfinate impurity. Spectra are internally referenced to TMS. Note that these spectra were recorded using a 600 MHz spectrometer, resulting in excellent resolution of the complex splitting pattern expected for this higher order spin system.

## Effect of the presence of oxygen on the reaction of CblOH with PA

To obtain information about the influence of oxygen on the reaction between CblOH and PA in alkaline solution, the reaction was also investigated under aerobic conditions and in the presence of varying concentrations of oxygen in solution. The reactions were initiated by the addition of a buffered solution of CblOH (pH 10.2, 0.10 M carbonate buffer, 25 °C) to an aqueous solution of PA. UV-Vis spectral changes observed for this reaction are shown in Figure S2a. Figure S2b shows the corresponding plot of absorbance at 535 nm as a function of time. The spectra once again show that there is a clean reaction between CblOH ( $\lambda_{\text{max}} = 357, 420, 509, 536 \text{ nm}$ ) and PA to produce CblNO ( $\lambda_{\text{max}} = 321, 480 \text{ nm}$ );<sup>[1,2]</sup> however, several reaction steps occur. The apparent induction period is significant compared with anaerobic experiments, and may suggest that initially redox cycling occurs during which dioxygen is used up.

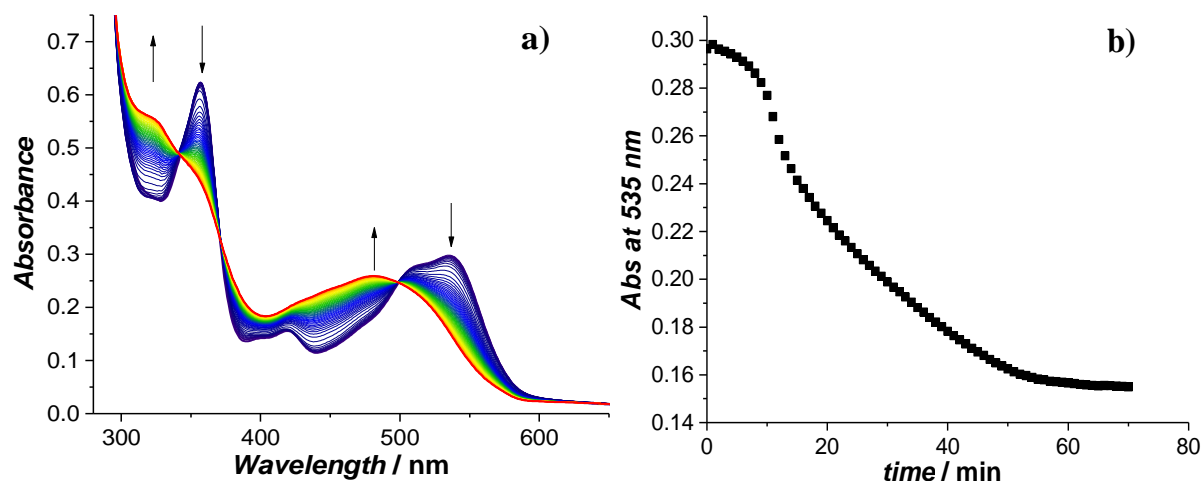
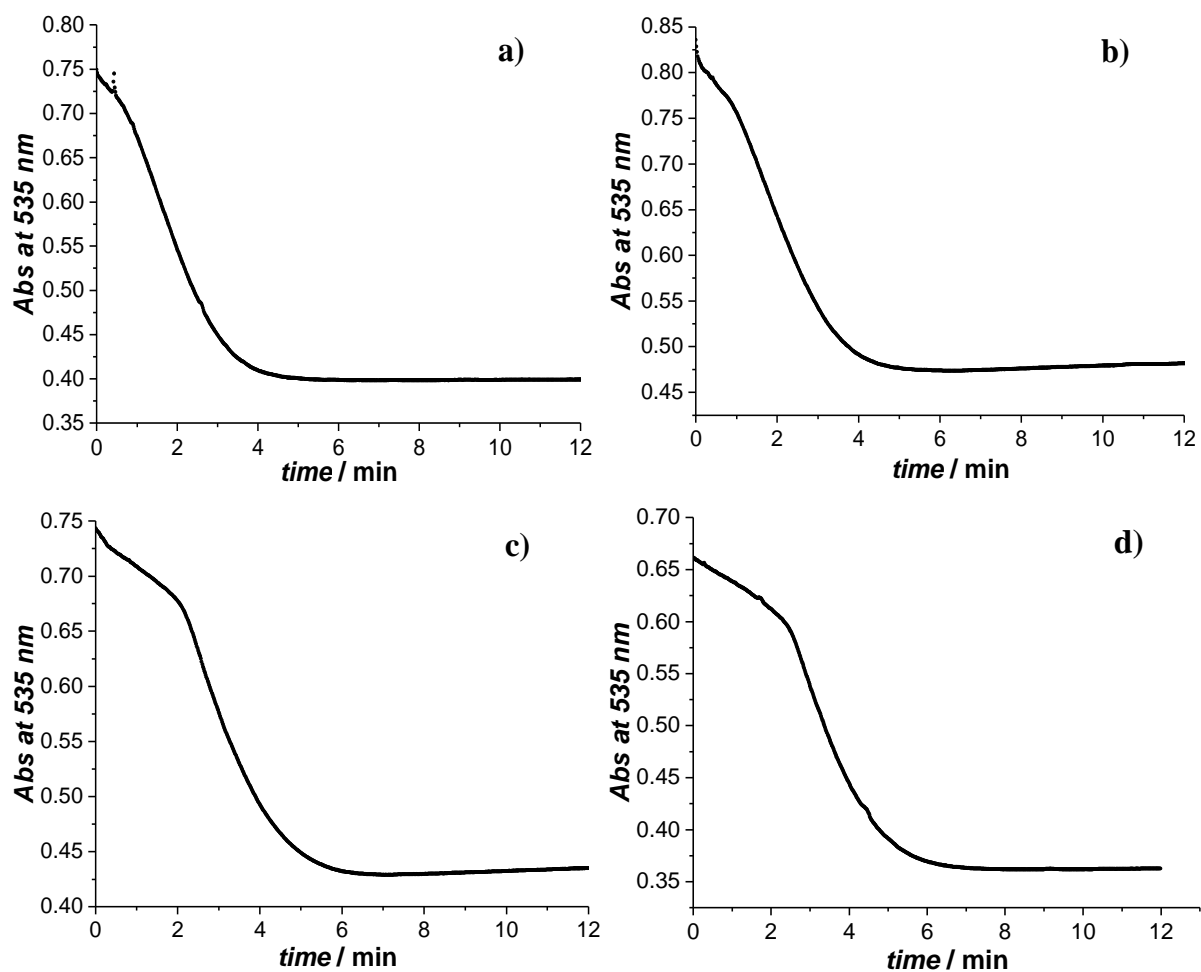


**Figure S2.** a) UV-Vis spectral changes observed for the reaction of CblOH with Pilyoty's acid. b) Plot of absorbance at 535 nm vs. time. Experimental conditions: [CblOH] =  $4.3 \times 10^{-5} \text{ M}$ , [PA] =  $2.2 \times 10^{-3} \text{ M}$ , pH 10.2 (0.10 M carbonate buffer), 25 °C, aerobic solution.

A series of experiments were performed where additional oxygen was introduced into the system. The results (Figure S3a-d) clearly show that the apparent induction period increases upon increasing the oxygen concentration. The steepest slope of the subsequent reaction does not appear to be affected by the oxygen concentration. These results suggest that the formation of CblNO is delayed by the presence of oxygen. Given that CblNO reacts rapidly with  $\text{O}_2$  to form CblOH and CblNO<sub>2</sub>,<sup>[1]</sup> it is likely that this reaction accounts for the consumption of oxygen.



**Figures S3.** Plots of absorbance at 535 nm vs. time. Experimental conditions:  $[CbI(OH)] = 8.5 \times 10^{-5} M$ ,  $[PA] = 4.3 \times 10^{-3} M$ , pH 10.2 (0.10 M carbonate buffer), 25 °C. Oxygen concentrations: **a)**  $2.1 \times 10^{-6} M$ , **b)**  $4.1 \times 10^{-6} M$ , **c)**  $1.7 \times 10^{-5} M$ , **d)**  $3.4 \times 10^{-5} M$ .

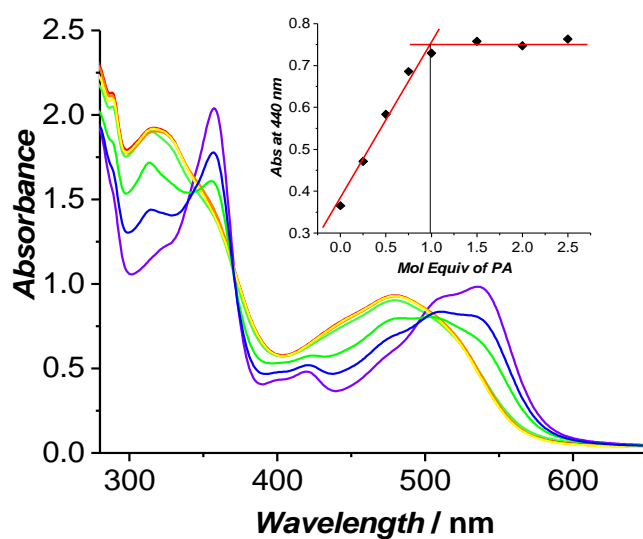


**Figure S4.** UV–Vis spectra for equilibrated anaerobic solutions of CblOH with 0–2.5 mol equiv. PA at pH 12.0 (0.10 M phosphate buffer, 25.0 °C). The concentration of CblOH was  $6.00 \times 10^{-3} M$  and the product solutions were diluted to  $1.00 \times 10^{-4} M$  inside a glove box before recording the UV–Vis spectra. Inset: Plot of absorbance at 440 nm versus mol equiv. PA for the same reaction.

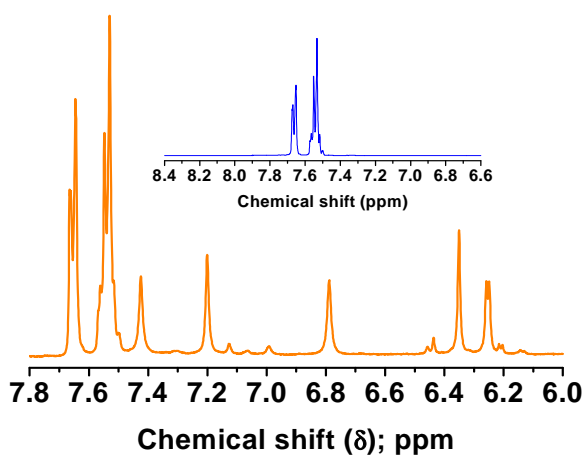


**Figure S5.** Aromatic region of the  $^1\text{H}$  NMR spectrum of the products of the reaction between CblOH ( $5.00 \times 10^{-3} \text{ M}$ ) and 1.1 mol equiv. PA at pD 12.0 (0.10 M phosphate buffer) under anaerobic conditions. The peaks at 7.43, 7.20, 6.79, 6.35 and 6.25 ppm correspond to CblNO<sup>[3]</sup> and those at 7.66, 7.65, 7.56 and 7.53 ppm correspond to benzenesulfinate. **Inset:**  $^1\text{H}$  NMR spectrum (aromatic region) for authentic sodium benzenesulfinate ( $\delta = 7.67, 7.65, 7.55$  and  $7.53$  ppm). The spectra are referenced to TSP (internal reference).

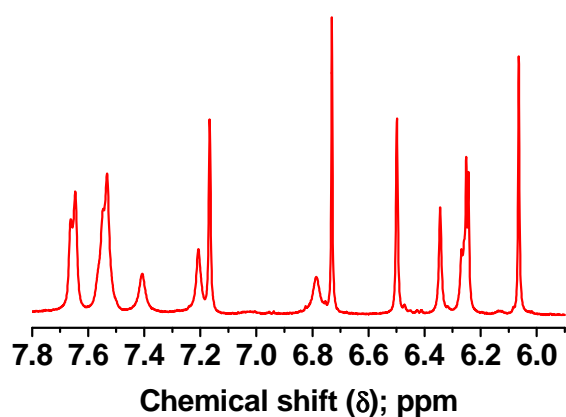


**Figure S6.** Aromatic region of the <sup>1</sup>H NMR spectrum of the products of the reaction between CblOH ( $6.00 \times 10^{-3} M$ ) and 0.5 mol equiv. PA at pD 12.0 (0.10 M phosphate buffer) under anaerobic conditions. The peaks at 7.66, 7.65, 7.55 and 7.53 ppm correspond to benzenesulfinate, those at 7.40, 7.21, 6.78, 6.34 and 6.25 ppm correspond to CblNO<sup>[3]</sup> and those at 7.17, 6.73, 6.50, 6.25 and 6.06 ppm correspond to unreacted CblOH. The spectra are referenced to TSP (internal reference).

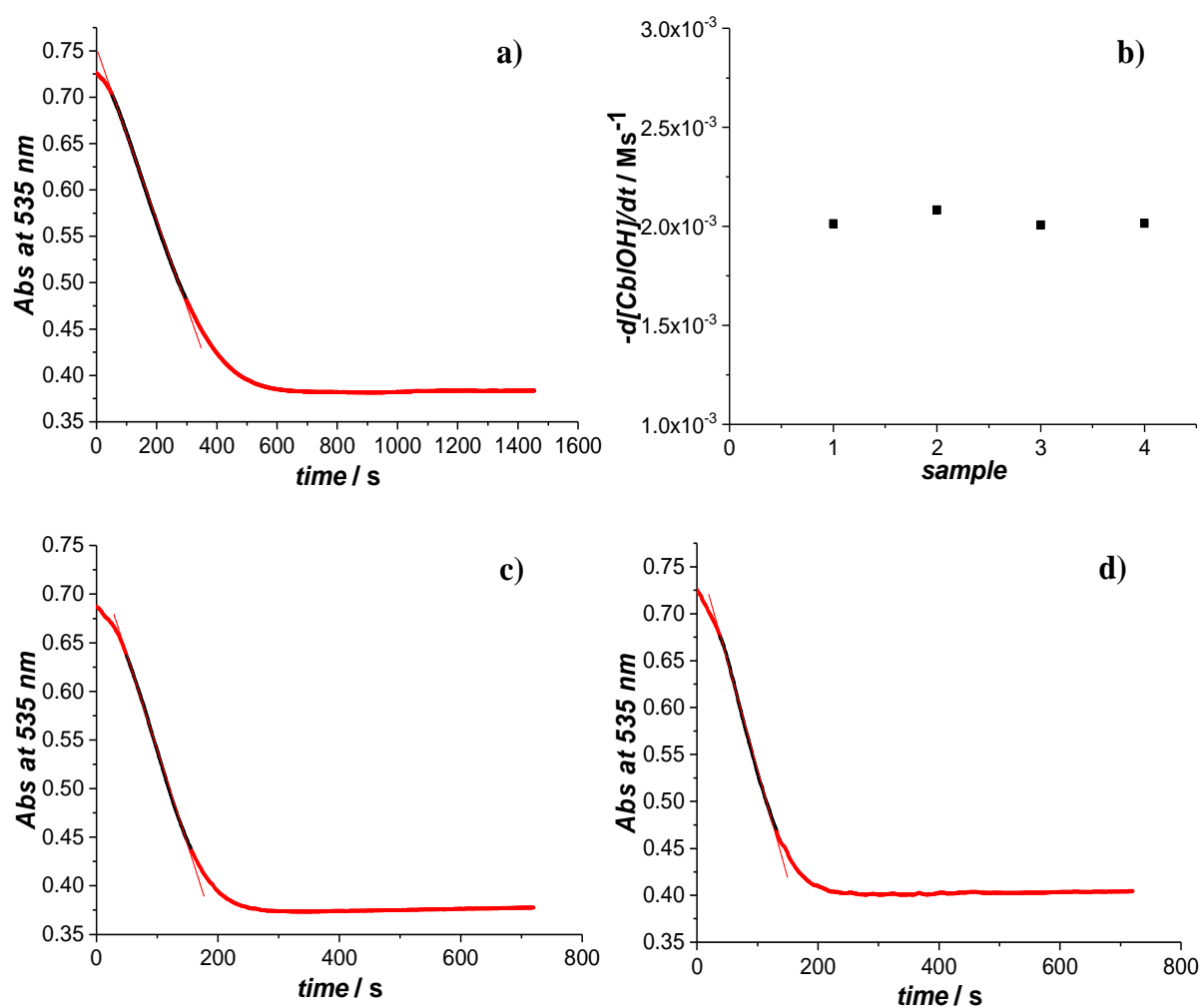


**Figure S7.** **a)** Plot of absorbance at 535 nm versus time for the reaction between CblOH ( $8.5 \times 10^{-5} M$ ) and PA ( $8.5 \times 10^{-4} M$ ) at pH 10.2 (0.10 M carbonate buffer, 25 °C, Ar atmosphere). The linear (steepest) part of the curve has a slope of  $(9.30 \pm 0.02) \times 10^{-4} M s^{-1}$ . **b)** Dependence of reaction rate on the experiment number. Experimental conditions: [CblOH] =  $8.5 \times 10^{-5} M$ , [PA] =  $4.2 \times 10^{-3} M$ , pH 10.0 (0.10 M carbonate buffer, 25 °C, Ar atmosphere). Plots of absorbance at 535 nm vs. time for the reaction between CblOH ( $8.5 \times 10^{-5} M$ ) and PA for **c)**  $4.2 \times 10^{-3} M$  and **d)**  $8.5 \times 10^{-3} M$ , at pH 10.2 (0.10 M carbonate buffer, 25 °C, Ar atmosphere). The linear (steepest) parts of the curves have slopes of **c)**  $(1.95 \pm 0.01) \times 10^{-3} M s^{-1}$  and **d)**  $(2.32 \pm 0.01) \times 10^{-3} M s^{-1}$ .



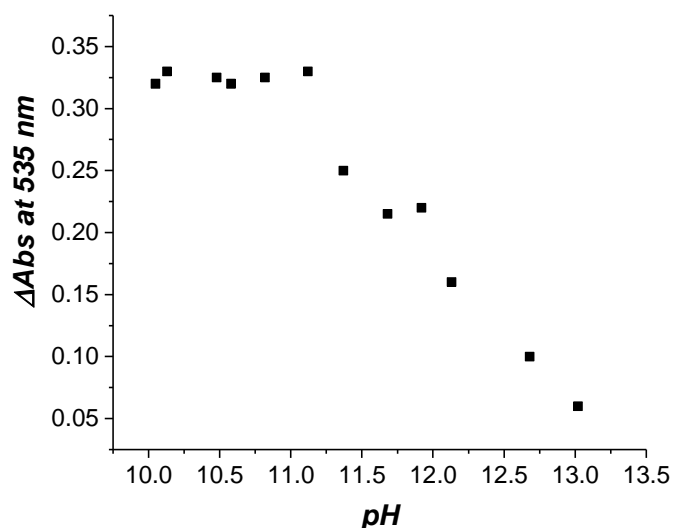


**Figure S8.** Plot of absorbance change at 535 nm versus pH for the reaction between CblOH ( $8.5 \times 10^{-5} M$ ) and PA ( $0.013 M$ ) as a function of pH ( $0.10 M$  buffer,  $25^\circ C$ , Ar atmosphere). Data were taken from the kinetic experiments at 60 min. From this data it is clear that the concentration of CblNO formed decreases as the pH is increased. In the higher pH range the final solution contains both CblNO and CblOH.

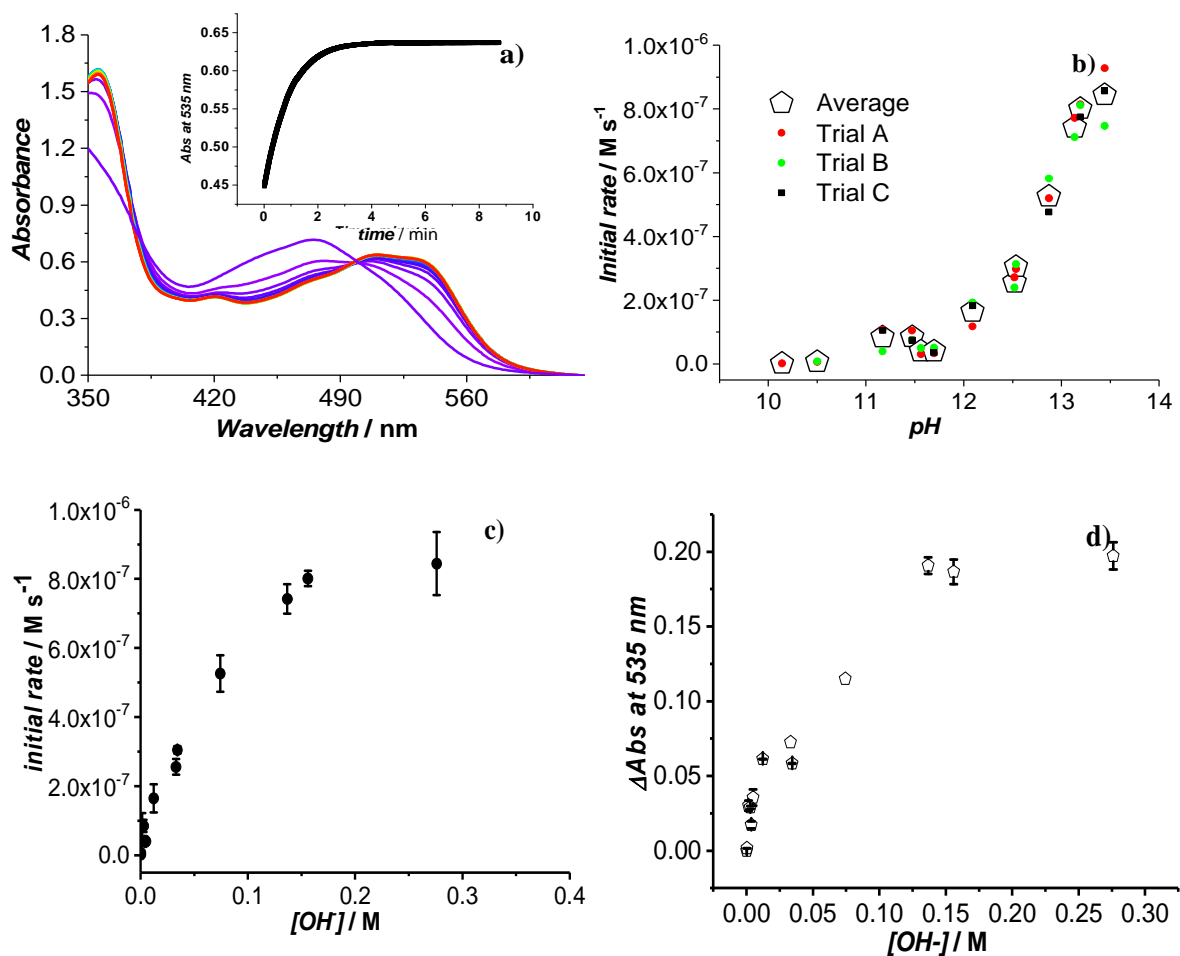


**Figure S9.** **a)** UV–Vis spectra for CblNO ( $7.8 \times 10^{-5} M$ ) upon the addition of PA ( $0.015 M$ ) in  $0.15 M$  NaOH ( $I = 1.0 M$  ( $\text{NaCF}_3\text{SO}_3$ )). The isosbestic points at  $375 \pm 3$  and  $499 \pm 1$  nm are consistent with CblNO reacting with  $\text{OH}^-$  to give CblOH. **Inset:** Plot of absorbance at 535 nm versus time for this data. **b)** Plot of the initial rate as a function of pH for the reaction between CblNO ( $7 \times 10^{-5} M$ ) and PA ( $0.015 M$ ) in anaerobic buffered solutions ( $0.20 M$  carbonate or phosphate buffer,  $I = 1.0 M$ ) or sodium hydroxide solutions ( $0.15$ – $0.35 M$ ,  $I = 1.0 M$ ). Initial rates were calculated by determining the initial slope of plots of change in concentration versus time ( $\Delta c = \Delta\text{Abs}/(\epsilon(\text{CblOH}) - \epsilon(\text{CblNO}))$ );  $\epsilon(\text{CblOH}) = 8260 M^{-1} \text{cm}^{-1}$  and  $\epsilon(\text{CblNO}) = 4430 M^{-1} \text{cm}^{-1}$  at 535 nm; determined by experiment. **c)** Plot of initial rate as a function of  $[\text{OH}^-]$  for the reaction between CblNO and PA under the same conditions as in **b)**. **d)** Change in absorbance at 535 nm as a function of  $[\text{OH}^-]$  for the reaction between CblNO and PA under the same conditions as in **b)**.

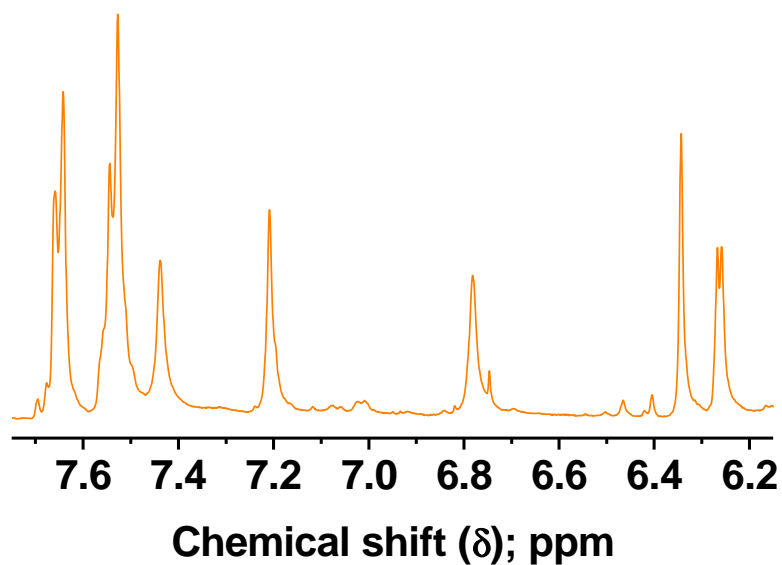


**Figure S10.** Aromatic region of the <sup>1</sup>H NMR spectrum of the products of the reaction between CblOH ( $6.00 \times 10^{-3} M$ ) and 1.1 mol equiv PA at pD 7.0 (0.10 M phosphate buffer) under anaerobic conditions. The peaks at 7.66, 7.64, 7.54 and 7.53 correspond to benzenesulfinate, those at 7.44, 7.20, 6.78, 6.34 and 6.26 ppm correspond to CblNO<sup>[3]</sup>

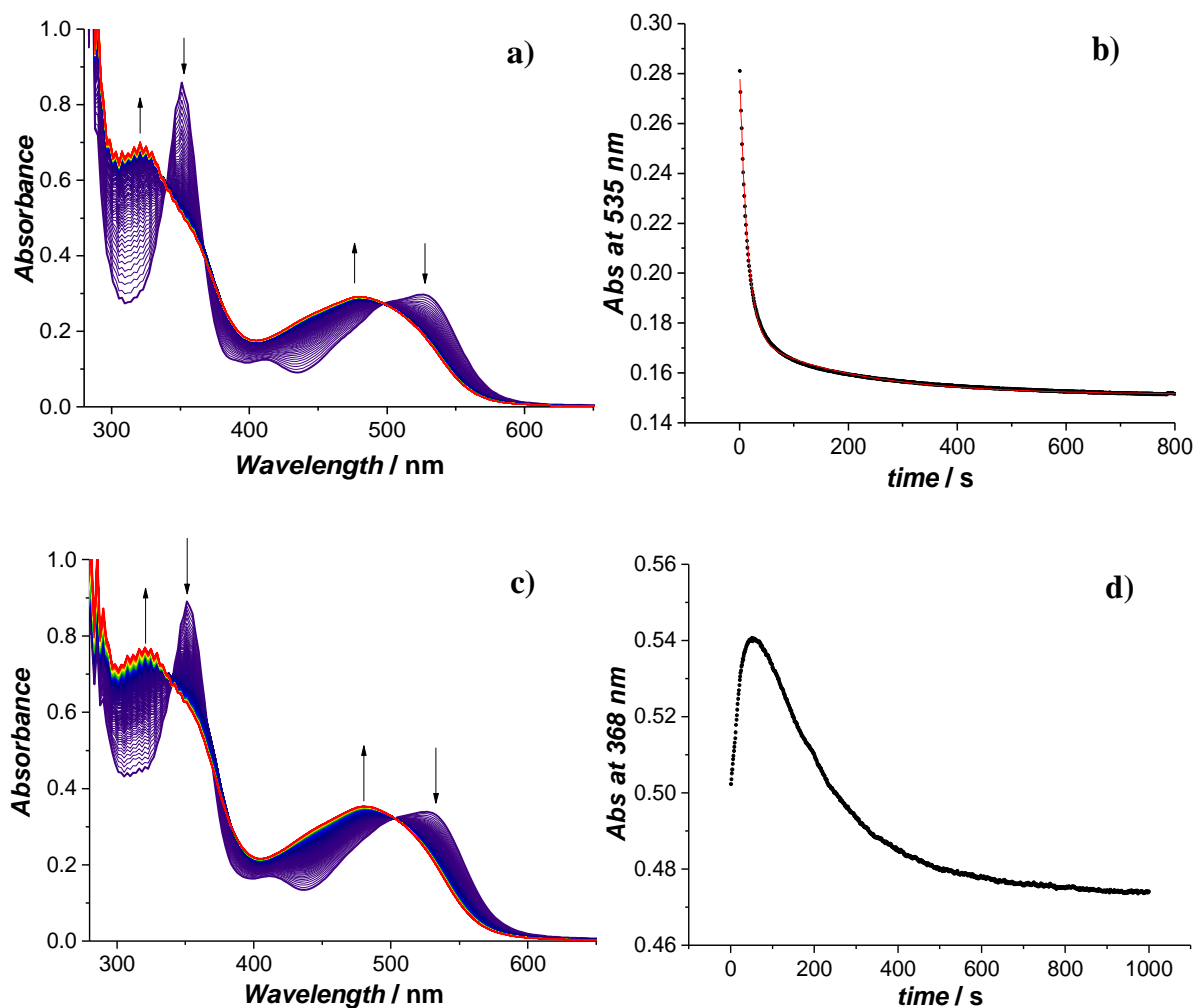


**Figure S11.** **a)** UV-Vis spectra recorded for the reaction between  $\text{CblOH}_2^+$  ( $4.3 \times 10^{-5} \text{ M}$ ) and PA ( $2.2 \times 10^{-3} \text{ M}$ ) at pH 7.2 (0.10 M Tris buffer, 25 °C, Ar atmosphere). Spectra recorded during the first 800 s. **b)** Typical kinetic trace recorded at 535 nm for the reaction between  $\text{CblOH}_2^+$  ( $4.3 \times 10^{-5} \text{ M}$ ) and PA ( $2.2 \times 10^{-3} \text{ M}$ ) at pH 7.2 (25 °C, 0.10 M Tris buffer). The data was fitted to a double exponential function for two parallel reactions, giving  $k_{\text{obs}1} = (70.6 \pm 0.3) \times 10^{-3} \text{ s}^{-1}$  and  $k_{\text{obs}2} = (5.12 \pm 0.04) \times 10^{-3} \text{ s}^{-1}$ . Experimental data – black curve; first-order fit – red curve (duplicated from Ref 53). **c)** UV-Vis spectral changes observed for the reaction between  $\text{CblOH}_2^+$  ( $4.3 \times 10^{-5} \text{ M}$ ) and PA ( $2.2 \times 10^{-3} \text{ M}$ ) in the presence of  $\text{PhSO}_2^-$  ( $4.3 \times 10^{-5} \text{ M}$ ) at pH 7.2 (0.10 M Tris buffer, 25 °C, Ar atmosphere, data recorded for 1000 s). **d)** Plot of absorbance at 368 nm versus time.

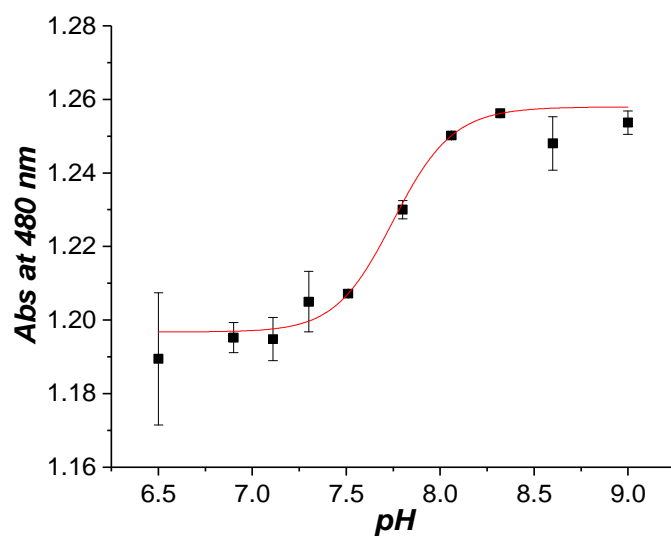


**Figure S12.** Plot of absorbance at 480 nm versus pH for the reaction between  $\text{CbIOH}_2^+/\text{CbIOH}$  ( $1.7 \times 10^{-4} \text{ M}$ ) and PA ( $8.6 \times 10^{-4} \text{ M}$ ) as a function of pH (0.10 M buffer, 25 °C, Ar atmosphere). Data were collected 60 minutes after the initiation of the reaction.

## References

- [1] Subedi, H.; Hassanin, H. A.; Brasch, N. E. Kinetic and Mechanistic Studies on the Reaction of the Vitamin B12 Complex Aquacobalamin with the HNO Donor Angeli's Salt: Angeli's Salt and HNO React with Aquacobalamin. *Inorg. Chem.* **2014**, *53*, 1570–1577.
- [2] Wolak, M.; Zahl, A.; Schnepf, T.; Stochel, G.; van Eldik, R. Kinetics and Mechanism of the Reversible Binding of Nitric Oxide to Reduced Cobalamin B<sub>12</sub> (Cob(II)alamin). *J. Am. Chem. Soc.* **2001**, *123*, 9780–9791.
- [3] Hannibal, L.; Smith, C.A.; Jacobsen, D.W.; Brasch, N.E. Nitroxylcob(III)alamin: synthesis and X-ray structural characterization. *Angew. Chem. Int. Ed. Engl.* **2007**, *46*, 5140–5143.